CONFIDENTIAL

Copy
RM E53C11

NACA

RESEARCH MEMORANDUM

INVESTIGATION OF A 10-STAGE SUBSONIC AXIAL-FLOW RESEARCH COMPRESSOR

IV - INDIVIDUAL STAGE PERFORMANCE CHARACTERISTICS

By Ray E. Budinger and George K. Serovy

Lewis Flight Propulsion Laboratory
Cleveland, Ohio

CLASSIFIED DOCUMENT

NATIONAL ADVISORY COMMITTEE
FOR AERONAUTICS

WASHINGTON
April 28, 1953

CONFIDENTIAL

NATIONAL ADVISORY COMMITTEE FOR AERONAUTICS

RESEARCH MEMORANDUM

INVESTIGATION OF A 10-STAGE SUBSONIC AXIAL-FLOW RESEARCH COMPRESSOR

IV - INDIVIDUAL STAGE PERFORMANCE CHARACTERISTICS

By Ray E. Budinger and George K. Serovy

SUMMARY

The individual stage performance was determined for a 10-stage axial-flow compressor from circumferentially fixed radial rake measurements of total temperature and total pressure obtained at the discharge of each stage. The intermediate speed range in which surge problems have been encountered in multistage axial-flow compressors was also investigated. The results of this investigation showed the existence of a slight knee in the compressor surge line between 70 and 74 percent of design speed. The interstage data indicated that the knee in the surge line and the corresponding drop in compressor total-pressure ratio before surge on the 70-percent speed curve appear to be directly associated with the positive stall of some inlet stage at low speeds and its effect through stage interactions on the performance of several of the succeeding stages and possibly some of the preceding stages. The magnitude of the knee in the compressor surge line probably is also affected by the type of stall initiated in the inlet stages of the compressor. The progressive tip-to-hub stall found in the early stages of this compressor at low speeds is better than a simultaneous root-to-tip stall because it reduces the effect of stall on the over-all compressor performance and probably tends to reduce the effect of stage interactions which are propagated axially through the compressor by means of an unstable rotating stall phenomenon.

INTRODUCTION

The use of high pressure ratio axial-flow compressors is posing serious starting and accelerating problems in current jet aircraft engines. The degree to which this problem exists in a given unit is approximately measured by the nearness of the equilibrium engine operating line to the compressor surge line. The distance between these lines is called the margin for acceleration of the engine. Two factors which reduce this margin are the inherently low compressor efficiency at low engine speeds and the change in slope of the compressor surge line at intermediate speeds. Both these factors are directly associated with the individual stages and the matching characteristics of these stages in the compressor.

Multistage axial-flow compressors are generally designed to obtain peak efficiency in all stages at a specified speed and pressure ratio. At speeds below design the exit stages limit the weight flow, causing high angles of attack and subsequent stall of the inlet stages. The high losses associated with blade stall seriously reduce the compressor efficiency at low speeds. At some intermediate point along the surge line there is a speed at which incipient stall will be encountered in some inlet stage. Reference 1 indicates that the knee in the surge line of one particular compressor was the result of the stalling of some inlet stage and the consequent effect, through stage interactions, of this stall on preceding and succeeding stages.

In order to determine the general applicability of the results of reference 1 and present additional data and further explanations of stage matching characteristics of multistage axial-flow compressors, an investigation similar to that of reference 1 was conducted at the NACA Lewis laboratory on the 10-stage research compressor reported in references 2 and 3. The surge line characteristics of the compressor reported in reference 1 and the 10-stage compressor reported herein exhibit the same general trend, although the magnitude of the knee in the surge line of the 10-stage compressor at intermediate speeds is considerably less and the part-speed efficiencies are much higher than for the 16-stage compressor of reference 1. An attempt to evaluate some of the factors which affect the shape of the surge line may thus be afforded by use of the stage performance curves presented herein and stall data obtained on the 10-stage compressor which are presented in reference 4.

Circumferentially fixed radial rake measurements of total temperature and total pressure were obtained after each stage for a range of flows from choke to surge over a range of speeds from 50 to 100 percent of design speed. The individual stage performance and over-all compressor performance were evaluated from these measurements and are presented herein.

APPARATUS AND INSTRUMENTATION

The 20-inch tip diameter, 10-stage axial-flow compressor reported in references 2 and 3 and schematically shown in figure 1 was used for the investigation. The test installation and instrumentation for the determination of the over-all compressor performance are the same as those presented in reference 3. In addition, interstage instrumentation was installed at the axial stations shown in figure 1. After each stator blade row a single radial total-pressure rake (fig. 2(a)) and a single radial total-temperature rake (fig. 2(b)) were used for the determination of the individual stage performance. Locating the rakes behind stator rows where the discharge flow angle remains relatively constant over a wide range of flow conditions would tend to minimize flow angularity effects on the instrument measurements. The rakes in

the first five stages had five measuring tips each and the rakes in the last five stages had three measuring tips. Area centers of equal annular areas were used to determine the radial location of the measuring tips on each rake. Consideration was given to locating instruments around the periphery of the compressor such that they would be free of upstream instrument and blade wakes. The pressure measurements were photographed from mercury manometers and the stage temperatures were measured differentially with thermocouples in the depression tank on a calibrated self-balancing potentiometer.

PROCEDURE

The compressor was operated at speeds from 50 to 100 percent of equivalent design speed. At each speed a range of air flows was investigated from a maximum flow at which the compressor was choked to a minimum flow at which surge occurred. The design speed surge point was not obtained because of mechanical difficulties with the test rig. The inlet pressure was varied to maintain a constant Reynolds number of approximately 190,000 relative to the first rotor at all speeds. The Reynolds number is defined as $\rho V l/\mu$, where the characteristic length l is the chord length at the tip of the first rotor; the remaining symbols are defined in appendix A. The value of Reynolds number was chosen on the basis of the horsepower available to drive the compressor with a given gear ratio at an overspeed operating condition.

The over-all compressor performance characteristics were calculated from the inlet weight flow, the total pressure and temperature, and the discharge static pressures, total temperatures, and the necessary fluid flow equations as recommended in reference 5. This method is the same as that used in the presentation of the calculated data in the preliminary over-all performance investigation of reference 3 which does not credit the compressor with nonuniformities of outlet flow velocity and deviation from axial discharge.

The individual stage performance was determined from arithmetic averages of total pressure and total temperature at the discharge of each stage in conjunction with the tables of reference 6. The stage performance is presented in terms of flow coefficient, equivalent pressure ratio, equivalent temperature-rise ratio, and adiabatic efficiency. Complete derivations of these dimensionless performance parameters can be found in reference 1. The stage performance data presented in reference 1 omitted the Mach number term in the flow coefficient parameter. Inasmuch as the scatter of the data can be reduced by including the Mach number term, an approximate Mach number was determined from the outer wall static pressure and average total pressure at the entrance to each stage for the data presented herein. The exact forms of the parameters as used to calculate the individual stage performance of the compressor are presented in appendix B.

The flow range of any given stage in a multistage compressor cannot be controlled independently of speed because of the choke and surge limits imposed on the compressor at any one speed. The stage performance parameters are a means of correlating the stage data independent of speed. The equivalent values presented are approximately those that would have been obtained if the complete flow range of each stage could have been covered at design speed.

The flow coefficient Q/UA is the ratio of the volume flow divided by the tip speed and annulus area at the entrance to the stage. The flow coefficient is equivalent to the ratio of mean axial velocity over tip speed and, consequently, it represents an average angle of attack on a stage. An increasing flow coefficient corresponds to a decreasing angle of attack and vice versa.

The absolute magnitudes of the values of the individual stage performance parameters are subject to errors for the following reasons:

1. The magnitudes of the temperature and pressure rises across a single stage are small, particularly at low compressor speeds.

2. The accuracy of the fixed rake instrumentation decreases when the flow angle deviations exceed $\pm 10^{\circ}$.

3. The location of the stator blade wakes varies both circumferentially and radially with changes in speed and weight flow. At some flow conditions it is probable that rakes in various stages may have been measuring partly or wholly in wake regions.

4. The measurements obtained in the high loss regions encountered behind a stalled blade row are questionable, as indicated in reference 7. Steady-stage instrumentation cannot accurately evaluate the unsteady flow disturbances set up by a stalled blade row. At the higher speeds, where all stages are operating unstalled and near their respective design discharge flow angles, the equivalent total-pressure and equivalent total-temperature-rise ratios should be reasonably accurate; however, very slight errors in the magnitude of either of these parameters have a considerable effect on the stage efficiencies.

5. The arithmetic averaging of the data is indicative of performance when the stages are unstalled and the radial distributions of flow are uniform. Inasmuch as the discharge conditions for one stage are the inlet conditions for the succeeding stage, any discrepancies in the performance of one stage will be reflected in the performance of the succeeding or preceding stage.

The general shape of the stage performance curves and the locations of the peaks and break points probably are unaltered by the inaccuracies in the absolute magnitudes of the values obtained.

RESULTS AND DISCUSSION

Compressor Performance

Over-all performance characteristics. - The over-all performance characteristics of the compressor with interstage instrumentation are presented in figures 3 and 4 as plots of total-pressure ratio and adiabatic temperature-rise efficiency as functions of equivalent weight flow over a range of equivalent speeds from 50 to 100 percent of design speed. Since the design speed surge point was not obtained, the surge limit line was extrapolated using the original over-all performance data of reference 3 as a guide. This extrapolation (shown on fig. 3 as a dashed line) indicated a maximum total-pressure ratio of approximately 7.2 at an equivalent weight flow of approximately 52 pounds per second with an efficiency of 0.81. The maximum equivalent weight flow obtained at design speed was 55.2 pounds per second.

The peak efficiency as shown on figure 4 increased from a value of 0.70 at 50 percent of design speed to 0.82 at 90 percent speed and then decreased to 0.81 at design speed. The maximum total-pressure ratio and maximum weight flow obtained at design speed and the peak efficiency obtained at all speeds differ from the results presented in reference 3. The maximum total-pressure ratio and maximum weight flow were decreased from approximately 7.5 to 7.2 and from 56 to 55 pounds per second, respectively. The peak efficiency decreased over a range from approximately 5 points at 50 percent to 1 point at design speed. These differences can be attributed to the following factors:

1. The inlet guide vanes were replaced after a periodic blade inspection revealed fatigue cracks in the original vanes. The setting angle on the replacement vanes was in slight error in the direction of an increase with respect to the compressor axis.

2. Corrosion of the flow passages and blading after the use of refrigerated air necessitated the coating of these surfaces with heat-resistant aluminum paint. The surface finish effects on compressor efficiency exhibit the same general trends as those obtained in the single-stage compressor investigation of reference 8, that is, the peak efficiency decreases with decreasing speed and the efficiency also decreases with increasing flow at a given speed.

3. The interstage instrumentation introduced additional flow disturbances and area blockage which could affect the over-all compressor performance.

Surge characteristics. - In view of the surge problems encountered in the intermediate speed range on high pressure ratio axial-flow compressors, additional data were obtained at surge between 70 and 80 percent

of design speed. These results, shown in figure 3, indicate a slight knee in the surge line of the compressor that was not shown in the original investigation presented in reference 3. Since the original tests were run in 10 percent speed increments, it appeared that the surge line gradually changed slope between 70 and 80 percent of design speed. The change in slope in the surge line is characterized by a rapid increase in surge weight flow and compressor efficiency when plotted against increasing speed, as shown in figure 5. This trend is typical of high pressure-ratio axial-flow compressors; however, the severity of the surge limitation varies considerably with different compressors, as evidenced by the results of reference 1. The magnitude of the knee in the surge line of this compressor would not impose a serious restriction on the acceleration to design speed of an engine using this compressor. The acceleration time of the engine would also be good because of the high part-speed efficiencies. The analysis of the interstage data presented in the remainder of this report will attempt to find the reason the surge line is relatively smooth and low speed efficiencies are high for this compressor, whereas other axial-flow compressors have severe surge limitations in the intermediate speed range combined with low part-speed efficiencies.

Stage Performance

The qualitative analysis of stage matching and off-design performance presented in reference 9 gives an indication of the operating range of the individual stages in a multistage axial-flow compressor over a range of speeds and flows. This analysis, however, does not show the effects of stage interactions which the data of reference 1 indicate are an important factor in determining the magnitude of the knee in the compressor surge line. The type of stage performance characteristic and the effect of stage interactions will be discussed with respect to their effect on over-all compressor performance characteristics in the following sections.

Inlet stage performance. - The performance characteristics of the inlet stage are presented in figure 6(a). The equivalent performance parameters were evaluated from the compressor inlet conditions of total pressure and total temperature, and consequently the losses through the inlet bellmouth and guide vanes are included in the performance values of the inlet stage. The flow coefficient for this stage is based on the flow conditions and annulus area at the entrance to the first rotor. The inlet stage operates at least partially stalled (as shown in fig. 6(a)) below a flow coefficient of approximately 0.46, as evidenced by the rapidly rising equivalent temperature-rise ratio and the positive slope of the equivalent total-pressure-ratio curve at flows below this value. The surge points denoted by the tailed symbols indicate that the inlet stage becomes stalled along the surge line at approximately 74 percent of

equivalent design speed, which corresponds to the initial change in slope of the over-all compressor performance curves at surge shown in figure 5. At 70 percent of equivalent design speed the inlet stage operates unstalled when the compressor is choked but as the weight flow is decreased at that speed, the angle of attack increases to the point of positive stall of the stage. This fact is clearly shown by the rapid increase in the equivalent total-temperature-rise ratio of the 70 percent speed data points in figure 6(a) as the flow coefficient is decreased. The equivalent total-pressure ratio exhibits only a slight drop which is coincident with the rapid increase in equivalent total-temperature-rise ratio. The pressure producing capacity of the stage is not seriously reduced because of positive stall; however, the work input required to obtain this pressure rise increases rapidly, causing a sharp decrease in the efficiency of the first stage, as shown in figure 6(a). The shape of the over-all compressor performance curves at 70 percent speed on figures 3 and 4 reflects the effect of the inlet stage stall. The magnitude of these effects may be increased through stage interactions which affect the performance of succeeding stages. The shapes of the surge line and characteristic curves in the intermediate speed range appear to be governed by stall of the inlet stages. Because of the manner in which the individual stages operate in a high pressure ratio, multistage axial-flow compressor, stall of the inlet stages is unavoidable at low speeds unless a means of alleviating this stall condition, such as adjustable guide vanes and stator blades or air bleed, is incorporated into the mechanical design. The aerodynamic design using fixed blading may be compromised such that good low speed performance or good high speed performance will be obtained, depending on the ultimate use of the engine. Designing a compressor such that the inlet stage will stall at a lower speed by setting the blades at lower than design angles of attack will improve the low speed efficiencies of the compressor but, due to the limited range of the stage, will cause choking of the compressor weight flow at high speeds with a resultant decrease in performance. If the inlet stage were designed to stall at a higher speed the low speed efficiencies would decrease, thus increasing the starting problems and the acceleration time of a jet engine incorporating the compressor. The knee in the compressor surge line would probably be more severe for this type of design as a result of the occurrence of stall at a higher speed.

Performance of stages 2 to 10. - The second stage exhibits the same general equivalent performance characteristics as the inlet stage. The effects of stage stall are less severe for the second stage, as shown on the equivalent temperature-rise ratio and adiabatic efficiency curves of figure 6(b). The performance curves for stages three through five presented on figures 6(c) to (e) suggest a positive stall over approximately the same range of speeds and flows as the inlet stage stall. The stall in these stages is evident only in the equivalent total-pressure-ratio curve. The equivalent total-temperature-rise ratio and adiabatic

efficiency show little change over the entire range of flow coefficients for the third stage. The total temperature at the discharge of the fourth stage is probably in error, as shown by the very low efficiencies of this stage on figure 6(d) combined with impossible efficiencies which are over 100 percent for the fifth stage (fig. 6(c)). The performance curves (figs. 6(a) to (j)) indicate stall in the first five stages; beyond the fifth stage there is no evidence of stall. These results agree with the rotating stall investigation (ref. 4), which showed a rapid damping of the rotating stall as it passed through the fifth stage and very slight fluctuations in the latter stages. The performance of the second stage is adversely affected by stall of the inlet stage, as shown by the drop in efficiency at low values of flow coefficient in figure 6(b). This stall produces only a slight reduction in the equivalent total-pressure ratio and a negligible effect on the equivalent total-temperature-rise ratio of the next three stages. The flow coefficient for the first five stages increases with increasing speed, which corresponds to a decreasing angle of attack.

Stages six through eight (figs. 6(f) to (h)) operate over approximately the same range of flow coefficients and very near the peak of their stage equivalent total-pressure-ratio curves at all speeds. Consequently, these stages will operate close to peak efficiency under all speed and flow conditions.

Stages nine and ten (shown in figs. 6(i) and (j)) operate from the negative slope side of their equivalent stage total-pressure ratio curves toward peak pressure ratio with increasing speed and decreasing flow at a given speed. The flow coefficient for these stages decreases, indicating an increasing angle of attack with increasing speed. The flow coefficient for choke weight flow for stages nine and ten increases with decreasing speed. The compressor weight flow at the low and intermediate speeds is limited by a low angle of attack stall of one of the exit stages. Since the low angle of attack stall is affected by Mach number, it could be expected that the choke flow points would not fall on a single curve for these stages. Stages nine and ten approach the peak of their individual stage equivalent total-pressure ratio near surge at the higher compressor speeds (90 and 100 percent of design speed).

Individual stage operating range. - The maximum and minimum flow coefficients for each stage over the entire range of speeds and weight flows investigated are presented in figure 7. The difference between the maximum and minimum values is indicative of the range of flow coefficients or range of angle of attack of each stage. The fact that various stages have the same range of flow coefficients, however, does not necessarily mean that these stages operate over the same range of angle of attack. The variation of angle of attack with flow coefficient is dependent on the velocity diagrams of the individual stages. Since the design

velocity diagrams are similar for all ten stages of this compressor, a valid comparison of the operating range of each stage probably can be made from figure 7. The imposed flow range decreases from the inlet stage to a minimum at the entrance to the seventh stage and then increases rapidly in the exit stages. The fact that the minimum range occurred at the entrance to the seventh stage could be expected from the analysis of reference 9, which indicated that the minimum angle of attack range will occur in some stage between the middle and exit stages of a multistage compressor. The rapid increase in flow range of the exit stages indicates that these stages would be operating over the widest range of angle of attack; however, it is evident from the stage performance curves (fig. 6) that the inlet stages operate over the widest range of angle of attack. The inlet stages operate far into the positive stall region at low speeds and approach turbining at high speeds, whereas the exit stages operate only from choke to peak pressure ratio over the same range of compressor inlet flow conditions. The fact that the wide range of flow coefficient of the exit stage indicated on figure 7 is not a good indication of the angle of attack range can probably be attributed to the high Mach numbers at which these stages operate near choke flow in the low and intermediate speed range. The choke flow coefficient decreases considerably with increasing speed for the latter stages, as shown on figures 6(i) and (j).

Correlation of aerodynamic data and hot-wire anemometer data. - The hot-wire anemometer data obtained on this compressor and presented in reference 4 indicate the existence of rotating stall at 50, 60, and 70 percent of equivalent design speed. The aerodynamic data presented in this report indicate positive stall of the inlet stages at the same speeds. An attempt was made to determine which stage initiates stall in the inlet stages by correlating the flow coefficient at stall obtained from the hot-wire anemometer and aerodynamic data independent of speed for the first five stages. The very small change in flow coefficient of adjacent stages at the same inlet weight flow combined with the difficulty in determining the point of initiation of rotating stall (because of the initial instability of the phenomenon) made it impossible to determine which stage was the instigator of stall. In general, however, the aerodynamic data presented in figure 6 indicate positive stall, as evidenced by a drop in equivalent stage total-pressure ratio at a higher flow coefficient than the rotating stall of reference 4 detected by means of hot-wire anemometers.

Radial distributions downstream of first stage. - The radial distributions of total pressure and total temperature downstream of the first stage will show the effects of the wide range of operation of this stage on the over-all compressor performance. During the investigation the inlet stage reached a maximum angle of attack at surge at 50 percent speed, an optimum angle of attack for peak efficiency at 90 percent speed, and a minimum angle of attack at choke flow at design speed. Radial

distributions of measured total-pressure and total-temperature ratios across the inlet stage are presented for these three flow conditions on figure 8. The curves show the effects of positive stall of the inlet stage at the flow condition for maximum angle of attack, the essentially uniform radial distribution of total-pressure and total-temperature ratios at the peak efficiency point, and the near-turbining condition for the weight flow at minimum angle of attack. Positive stall is characterized by a decreasing total pressure and an increasing total temperature toward the tip, which indicates a tip stall of the stage at low speeds. The near-turbining condition at the minimum angle of attack results in a decrease in both total-pressure and total-temperature ratios and ultimately causes a low angle of attack stall and limits the compressor weight flow. The mean radius data point on the total-pressure ratio curve is not shown because the pressure reading was in obvious error because of a plugged instrument. The rapid change in flow conditions at the discharge of the first stage in the tip region indicates that the rate of change of angle of attack with flow for the tip blade sections may be very critical. Since the inlet stage is close to its choke point at design speed, very little increase in weight flow would be obtained when operating at speeds above design. The overspeed curve presented in reference 3 for this compressor bears out this effect.

Radial distributions of total-pressure and total-temperature ratios at surge are presented in figures 9(a) and (b), respectively. The decrease in total-pressure ratio and increase in total-temperature ratio in the tip region indicate the existence of stall along the surge line in the inlet stage at speeds of approximately 80 percent of design and below. As the speed is reduced below 80 percent of design, the stall condition progresses inward toward the hub of the compressor. At the low speeds (50 and 60 percent of design) the inlet stage is stalled over half the passage height at surge. Hot-wire anemometer data obtained at the tip, mean, and hub blade sections at the discharge of the first rotor and presented in reference 4 show the same trend. The magnitude of the weight flow fluctuations is greatest at the tip, diminishes gradually toward the mean radius, and is practically negligible at the hub. The effect of this tip stall condition is very slight when presented on the equivalent total-pressure-ratio curve in figure 6(a). Once tip stall occurs the equivalent total-pressure ratio of the inlet stages decreases very gradually with decreasing speed and with decreasing weight flow at a given speed. This characteristic can probably be attributed to the progressive stall of the inlet stage. As the stall progresses inward from the tip toward the root of the blade, the weight flow is forced to pass around the stalled region. Since the weight flow must be passed by an effectively reduced area, the axial velocity will increase in the hub region such that a nearly constant angle of attack will be maintained, thus preventing these blade sections from stalling. Consequently, the pressure producing capacity of the blade sections toward the hub will remain high after the incurrence of tip stall, which accounts for the gradual reduction in equivalent total pressure of the inlet stage shown on figure 6(a).

Blade element equivalent total-pressure ratio and equivalent total-temperature-rise ratio plotted against speed are presented in figure 10 for the inlet stage. The speeds along the surge line at which the various blade elements become stalled are evident from these curves. Radial position a, near the tip (fig. 10(a)), indicates the incurrence of stall along the surge line as the speed is reduced at approximately 78 percent of equivalent design speed. The work input or equivalent total-temperature-rise ratio for this blade element does not show an appreciable increase until the speed is reduced to 74 percent of design. At the next radial position toward the hub (fig. 10(b)), the drop in equivalent total-pressure ratio and the rise in equivalent total-temperature-rise ratio occur at 74 percent of equivalent design speed. The fact that the equivalent total-temperature-rise ratio indicates stall of the blade elements at radial positions a and b at the same speed accounts for the rapid increase in slope of this performance parameter in figure 6(a) at flow coefficients below a value of 0.46. Radial position c near the mean radius (fig. 10(c)) indicates stall along the surge line at speeds of 71 percent of design and below. The radial positions near the hub (figs. 10(d) and (e)) show that these blade elements are operating near peak total-pressure ratio or on the negative slope side of the equivalent blade element total-pressure-ratio curve. Consequently, these blade elements are operating unstalled and near peak blade element efficiency at flow conditions at which the blade elements toward the tip are stalled. The progressive tip-to-hub type of stall found in the inlet stage appears to be favorable because it maintains a relatively high pressure ratio at stall and causes more gradual changes in stage performance than a simultaneous root-to-tip stall. The stage interaction effects associated with a progressive type stall are probably less severe than for a stage which stalls simultaneously along the entire blade height because this latter type of stall would cause an abrupt discontinuity in the stage performance rather than the more gradual changes initiated by the progressive type of stall. The single-stage performance curves presented in reference 10 indicate the relative magnitude of the drop in total pressure for the progressive type of rotating stall, in which the number of stalls increases with decreasing flow coefficient, and the single rotating stall associated with simultaneous stall along the entire blade height.

Concluding Remarks

The individual performance curves for all ten stages are very flat over the range of flow coefficients at which they are required to operate. The slight drop in equivalent total-pressure ratio of the first five stages which accompanies stall of the inlet stages results in a very slight knee in the compressor surge line. In contrast with this slight knee the results of a similar investigation of a 16-stage axial-flow compressor reported in reference 1 show a large knee in the compressor surge line at intermediate speeds. One reason for the large

difference in magnitude of the knee in the surge line of the two compressors may be the higher over-all total pressure of the compressor of reference 1. Another reason may be the much higher loading of the inlet stage of that compressor as compared with the loading of the first stage of the 10-stage compressor reported herein. The peak equivalent total-pressure ratio of the inlet stage of the 16-stage compressor was 1.28 as compared with 1.18 for the 10-stage compressor. Consequently, the positive stall of the inlet stage will have a greater effect on the over-all compressor total-pressure ratio for the more highly loaded stage. This effect will also be increased because stall of the inlet stage of the 16-stage compressor occurs at a higher percentage of design speed. Another reason may be the extent to which stage interactions affect the performance of the succeeding stages once the inlet stage stalls. Reference 1 indicates that the performance of the first six stages of the 16-stage compressor were adversely affected by stall of the inlet stage, whereas only the second stage appeared to be affected to any extent by stall of the first stage for the 10-stage compressor. The extent to which these stage interactions affect the performance of succeeding or preceding stages is probably associated with the type of rotating stall which appears to be initiated by some inlet stage. The hot-wire anemometer data obtained on the 16-stage compressor were much less complete than the data presented in reference 4 in that only the rotating stall frequency and the magnitude of the weight flow fluctuations at one radius were determined for a few axial measuring stations. The analysis of these data and pressure transducer data obtained at surge and presented in reference 10 indicate a single complete stall along the entire blade height existing in the 16-stage compressor prior to surge at low speeds. The progressive stall of the 10-stage compressor is accompanied by a relatively small drop in stage equivalent total-presssure ratio. The relatively large drop in pressure ratio of the inlet stages of the 16-stage compressor indicates a complete root-to-tip stall, as discussed in reference 11. The types of stall encountered in the two compressors may be the primary reason for the difference in magnitude of the knee in their surge lines.

SUMMARY OF RESULTS AND CONCLUSIONS

The following results and conclusions were obtained from an investigation of the individual stage performance of a 10-stage subsonic axial-flow research compressor:

1. A slight knee existed in the surge line of this compressor between 70 and 74 percent of equivalent design speed. The operating line of an engine utilizing this compressor probably would not pass through the surge region because the magnitude of the knee in the surge line is slight.

2. The knee that existed in the compressor surge line and in the 70 percent speed over-all compressor total-pressure ratio curve appeared to be directly associated with the positive stall of some inlet stage and its effect through stage interactions on preceding and succeeding stages.

3. The existence of a progressive type stall instead of the more sudden root-to-tip stall is favorable in that the stage performance decreases gradually, thus having less effect on the over-all compressor performance than a stage which stalls simultaneously along the entire blade height. In addition, the stage interaction effects may be lessened by a progressive type stall.

4. Stall of the inlet stage adversely affected the performance of the first five stages. The performance of the second stage was more seriously affected by stall of the inlet stage than of stages three through five.

5. The flow coefficient for the first five stages increased (decreasing angle of attack) with increasing speed. The next three stages operated over approximately the same range of flow coefficients at all speeds. The flow coefficient for the last two stages decreased (increasing angle of attack) with increasing speed.

6. The inlet stages operated in the positive stall region at low compressor speeds and approached a low angle of attack stall, thus limiting the weight flow at high speeds. The exit stages operated near turbining, limiting the weight flow at low speeds, and approached a positive stall at surge at high speeds.

7. The inlet and exit stages operated over the widest range of flow coefficients or angle of attack with the minimum range occurring at the entrance to the seventh stage.

8. The performance curves for all ten stages were very flat, indicating that the individual stages will operate near maximum pressure ratio and peak efficiency over most of the speed and flow range.

Lewis Flight Propulsion Laboratory
National Advisory Committee for Aeronautics
Cleveland, Ohio

APPENDIX A

SYMBOLS

The following symbols are used in this report:

A	annulus area, sq ft
c_p	specific heat at constant pressure, Btu/(lb)($^{\circ}$F)
H	enthalpy, Btu/lb
P	total pressure, in. Hg abs
Q	volume flow, cu ft/sec
R	gas constant
T	total temperature, $^{\circ}$R
U	tip speed, ft/sec
V	velocity relative to first rotor, ft/sec
W	weight flow, lb/sec
Y	pressure ratio function $\left[\left(\frac{P_n}{P_{n-2}}\right)^{\frac{\gamma-1}{\gamma}} - 1\right]$
z	radius ratio
γ	ratio of specific heats
δ	ratio of total pressure to standard sea-level pressure
η	adiabatic temperature-rise efficiency
θ	ratio of total temperature to standard sea-level temperature
μ	viscosity, lb/ft-sec
ρ	static density, lb/cu ft

Subscripts:

is	isentropic process
d	design conditions
e	equivalent, indicates that the parameter to which it is affixed has been corrected to design speed
n	station number
0	inlet depression tank
1	discharge of inlet guide vanes
3,5,7 . . . 19	designating instrument stations as shown in fig. 1 at exit of first, second, third . . . ninth stage stator blades
22	discharge of exit guide vanes

APPENDIX B

CALCULATION OF DIMENSIONLESS STAGE PERFORMANCE PARAMETERS

The flow range of any given stage in a multistage axial-flow compressor cannot be controlled independently of speed; therefore, a method of correlation of stage performance data independent of speed is necessary in order to analyze stage matching characteristics. Dimensionless stage performance parameters of flow coefficient, equivalent pressure ratio, and equivalent temperature-rise ratio are developed in reference 1. These parameters are presented in the form used for the calculation of the individual stage performance.

Flow coefficient. - The flow coefficient for each stage was determined from the orifice weight flow, the radially averaged total pressure, total temperature, annulus area at the inlet to the rotor, the compressor tip speed, and an approximate Mach number based on the ratio of the radially averaged total pressure to the average outer wall static pressure as follows:

$$\frac{Q}{UA} = \frac{WRT_{n-2}}{UAP_{n-2}} \left(1 + \frac{\gamma-1}{2} M_{n-2}^2\right)^{\frac{1}{\gamma-1}}$$

The n-2 subscript notation is valid for the calculation of the performance of stages two through nine. The inlet and exit guide vanes are included in the performance parameters for the first and tenth stages and consequently an n-3 subscript notation must be used in evaluating the performance of these stages.

Equivalent temperature-rise ratio. - Since the tables of reference 6 were used for these calculations the relation $\Delta H = c_p \Delta T$ was substituted in the equation of reference 1 with the following result:

$$\left(\frac{\Delta T}{T_{n-2}}\right)_e = \frac{T_n}{T_{n-2}} - 1.0 = \frac{\frac{\Delta T}{T_{n-2}}}{\left(\frac{U}{\sqrt{T_{n-2}}}\right)^2} \left(\frac{U}{\sqrt{T_{n-2}}}\right)_d^2 = K \frac{\Delta H}{U^2}$$

where

$$K = \left(\frac{U}{\sqrt{T_{n-2}}}\right)_d^2 \frac{1}{c_p}$$

Equivalent pressure-rise ratio. - The equivalent pressure rise ratio was determined similarly to the equivalent temperature-rise ratio as follows:

$$\left(\frac{P_n}{P_{n-2}}\right)_e = (Y_e + 1.0)^{\frac{\gamma}{\gamma-1}}$$

where

$$Y_e = K\frac{\Delta H_{is}}{U^2}$$

and γ is assumed constant at a value of 1.395.

Adiabatic stage temperature-rise efficiency. - The stage efficiency was computed as follows:

$$\eta = \frac{Y_e}{\left(\frac{\Delta T}{T}\right)_e} = \frac{\Delta H_{is}}{\Delta H}$$

Since the speed correction term is the same for both numerator and denominator in this equation, either the measured values or the equivalent values can be used to determine the efficiency.

REFERENCES

1. Medeiros, Arthur A., Benser, William A., and Hatch, James E.: Analysis of Off-Design Performance of a 16-Stage Axial-Flow Compressor with Various Blade Modifications. NACA RM E52L03, 1953.

2. Johnsen, Irving A.: Investigation of a 10-Stage Subsonic Axial-Flow Research Compressor. I - Aerodynamic Design. NACA RM E52B18, 1952.

3. Budinger, Ray E., and Thomson, Arthur R.: Investigation of a 10-Stage Subsonic Axial-Flow Research Compressor. II - Preliminary Analysis of Over-All Performance. NACA RM E52C04, 1952.

4. Huppert, Merle C., Costilow, Eleanor L., and Budinger, Ray E.: Investigation of a 10-Stage Subsonic Axial-Flow Research Compressor. III - Investigation of Rotating Stall, Blade Vibration, and Surge at Low and Intermediate Compressor Speeds. NACA RM E53C19.

5. NACA Subcommittee on Compressors: Standard Procedures for Rating and Testing Multistage Axial-Flow Compressors. NACA TN 1138, 1946.

6. Keenan, Joseph H., and Kaye, Joseph: Thermodynamic Properties of Air. John Wiley & Sons, Inc., 1947.

7. Herzig, H. Z., Hansen, A. G., and Costello, G. R.: Visualization of Secondary-Flow Phenomena in Blade Row. NACA RM E52F19, 1952.

8. Moses, Jason J., and Serovy, George K.: Effect of Blade-Surface Finish on Performance of a Single-Stage Axial-Flow Compressor. NACA RM E51C09, 1951.

9. Finger, Harold B., and Dugan, James F., Jr.: Analysis of Stage Matching and Off-Design Performance of Multistage Axial-Flow Compressors. NACA RM E52D07, 1952.

10. Huppert, Merle C.: Preliminary Investigation of Flow Fluctuations During Surge and Blade Row Stall in Axial-Flow Compressors. NACA RM E52E28, 1952.

11. Huppert, Merle C., and Benser, William A.: Some Stall and Surge Phenomena in Axial-Flow Compressors. Paper presented at Twenty-First Inst. Aero. Sci. meeting, New York (N.Y.), Jan. 26-29, 1953.

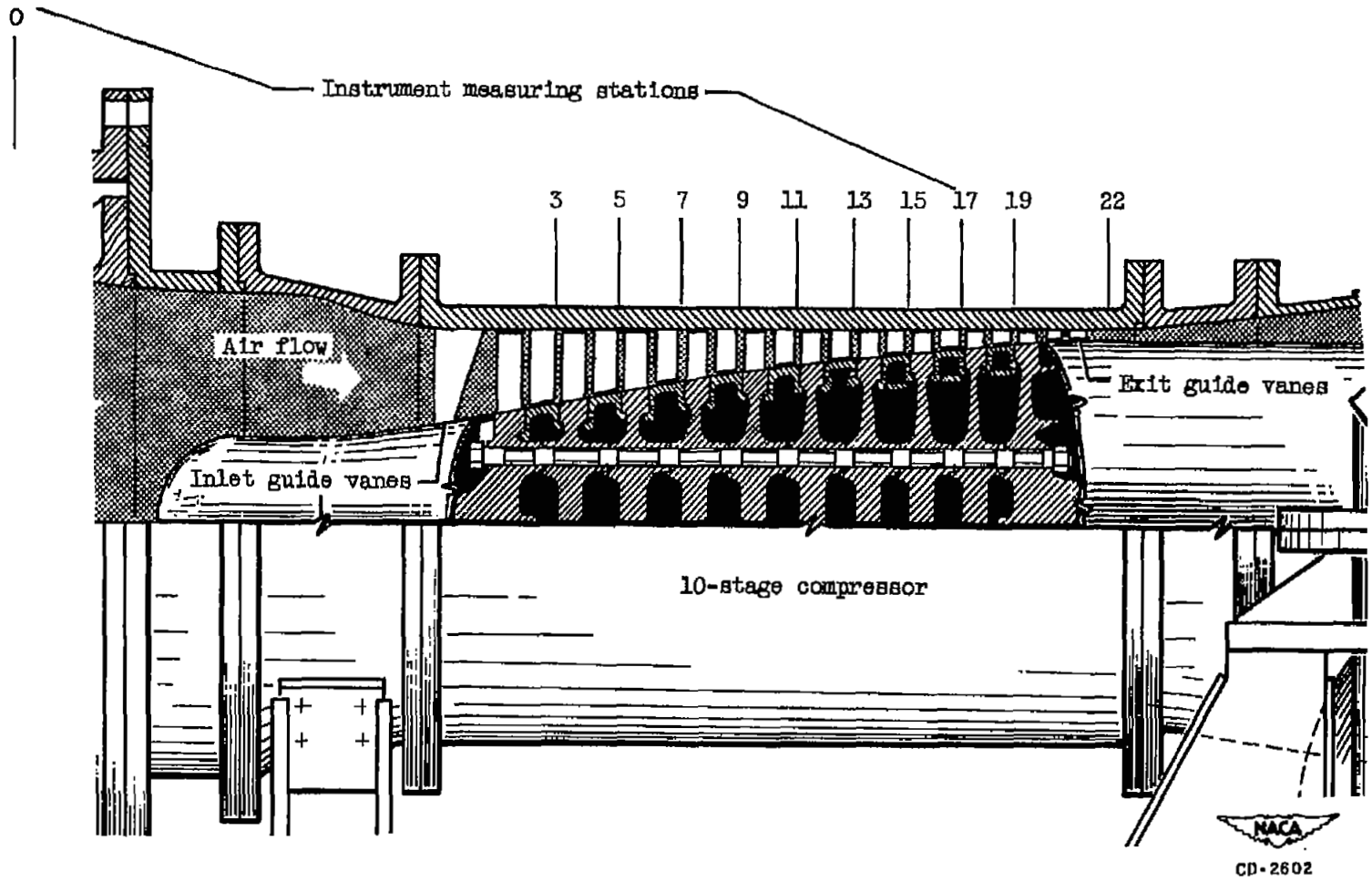

Figure 1. - Compressor cross section showing instrument measuring stations.

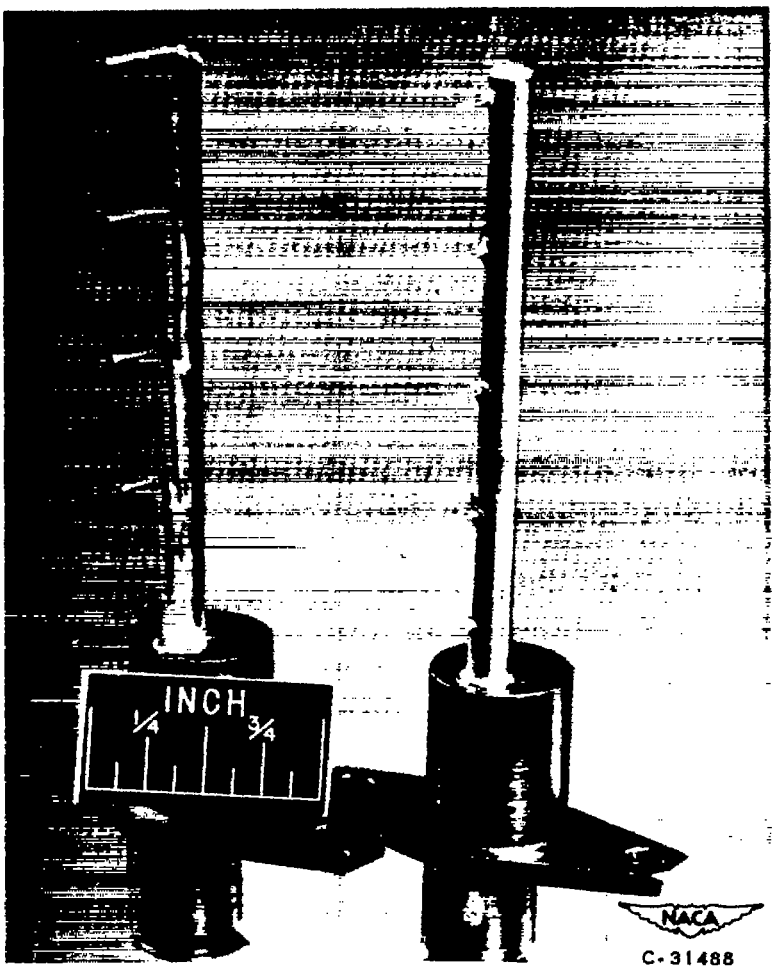

(a) Total-pressure rake (b) Spike-type total-temperature rake

Figure 2. - Typical radial rake instrumentation used for the determination of the stage performance characteristics.

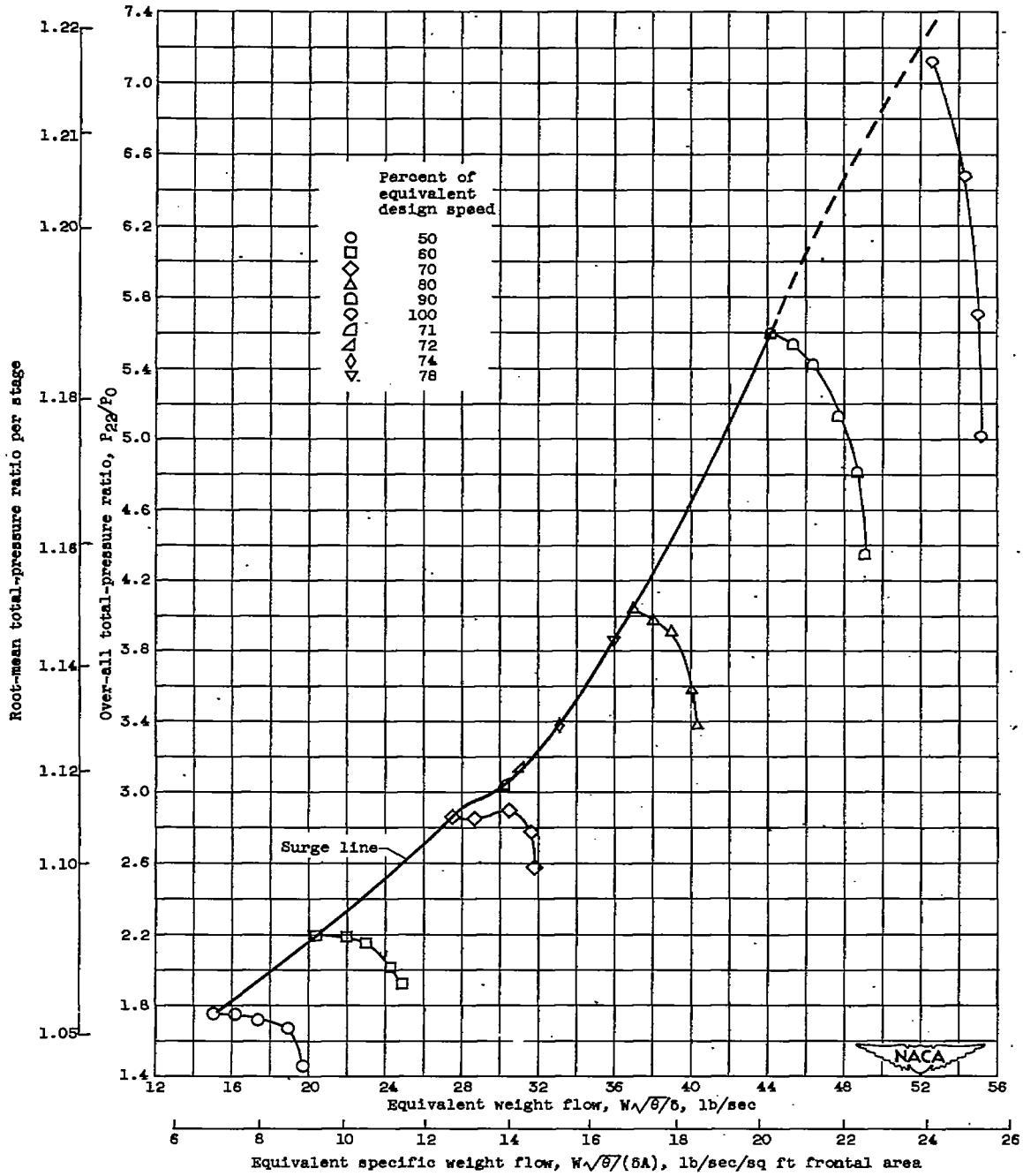

Figure 3. - Compressor total-pressure ratio over a range of weight flows at speeds from 50 to 100 percent of equivalent design speed.

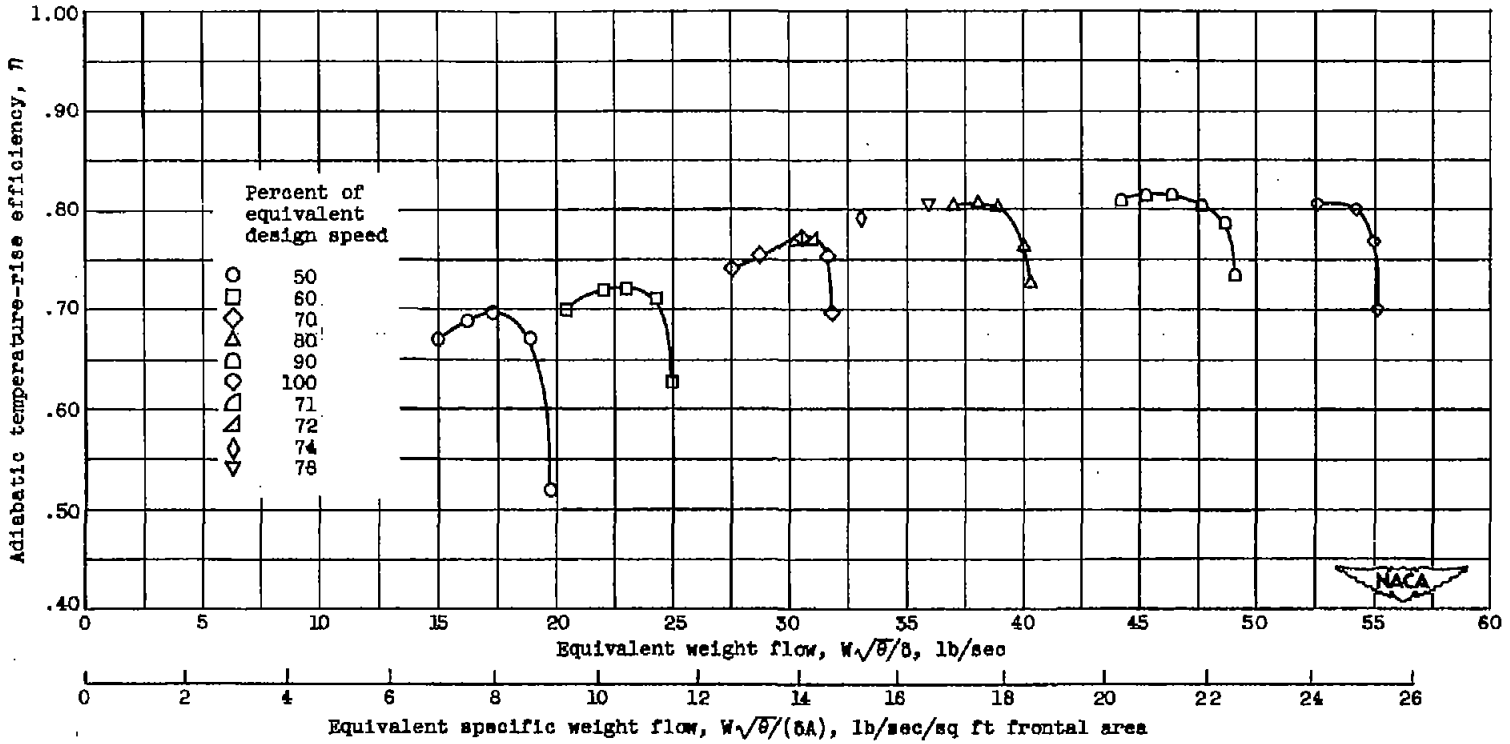

Figure 4. - Compressor adiabatic temperature-rise efficiency over a range of weight flows at speeds from 50 to 100 percent of equivalent design speed.

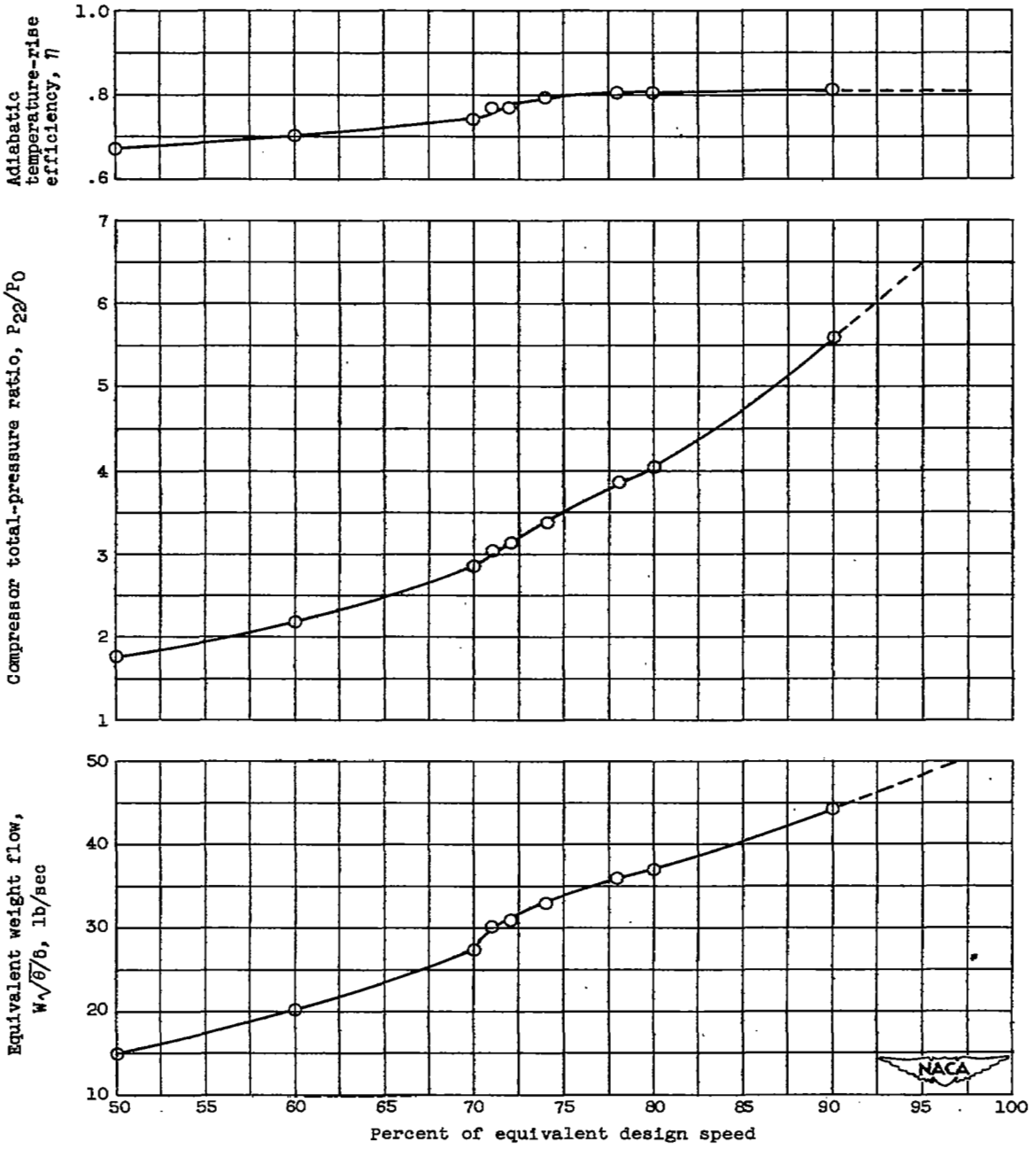

Figure 5. - Variation in over-all compressor performance at surge with speed.

[redacted]

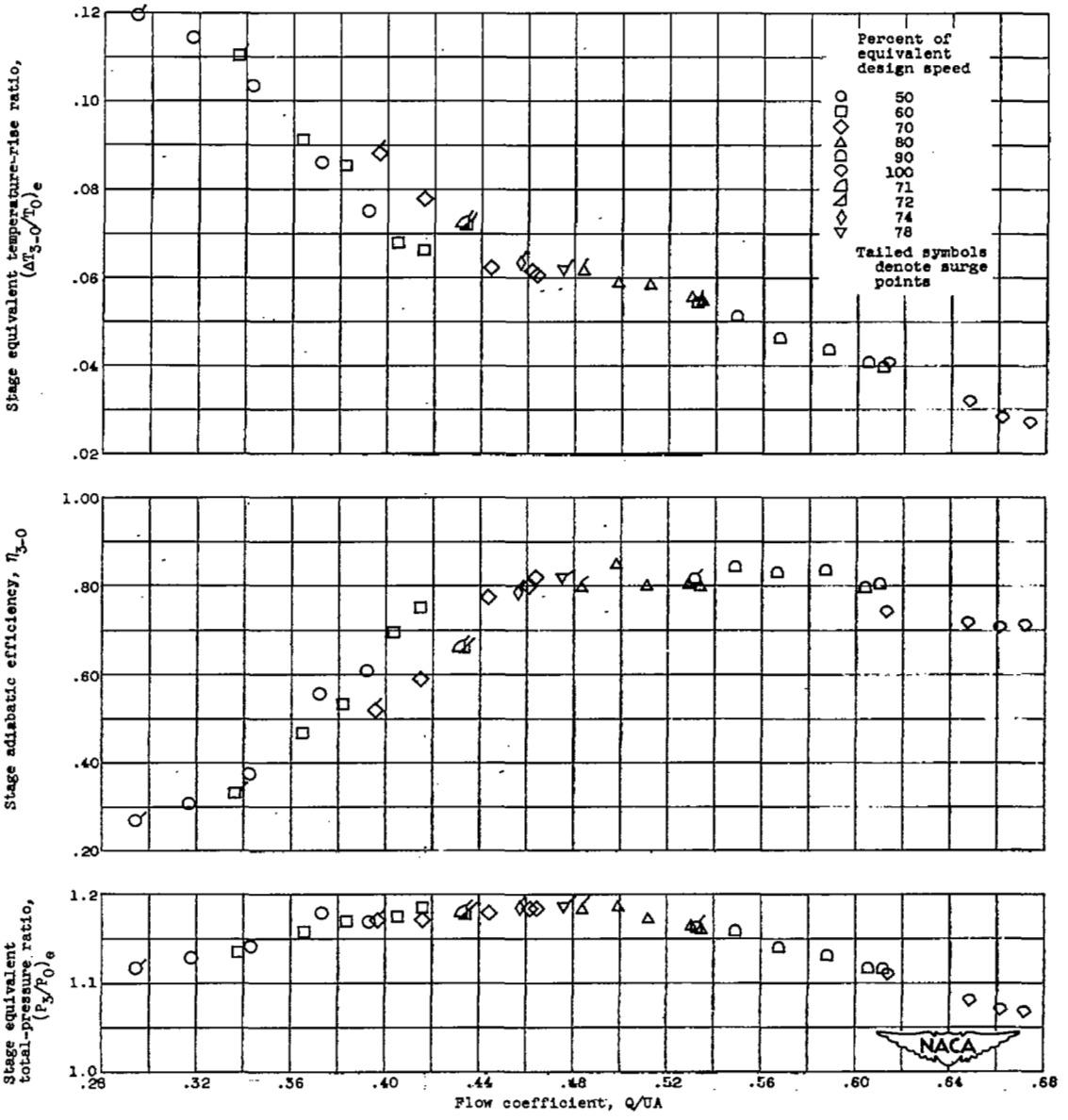

(a) First stage.

Figure 6. - Individual stage performance of 10-stage compressor over entire flow range at speeds from 50 to 100 percent of equivalent design speed.

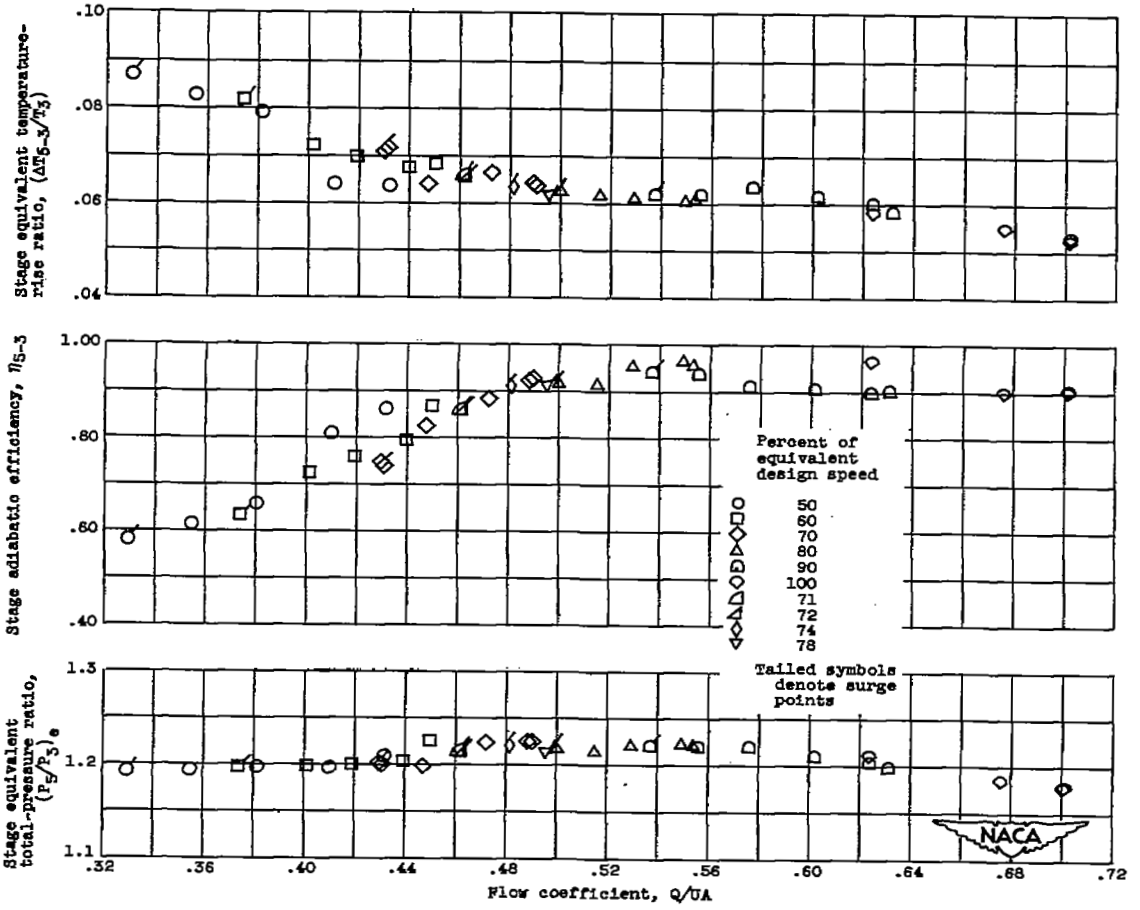

(b) Second stage.

Figure 6. - Continued. Individual stage performance of 10-stage compressor over entire flow range at speeds from 50 to 100 percent of equivalent design speed.

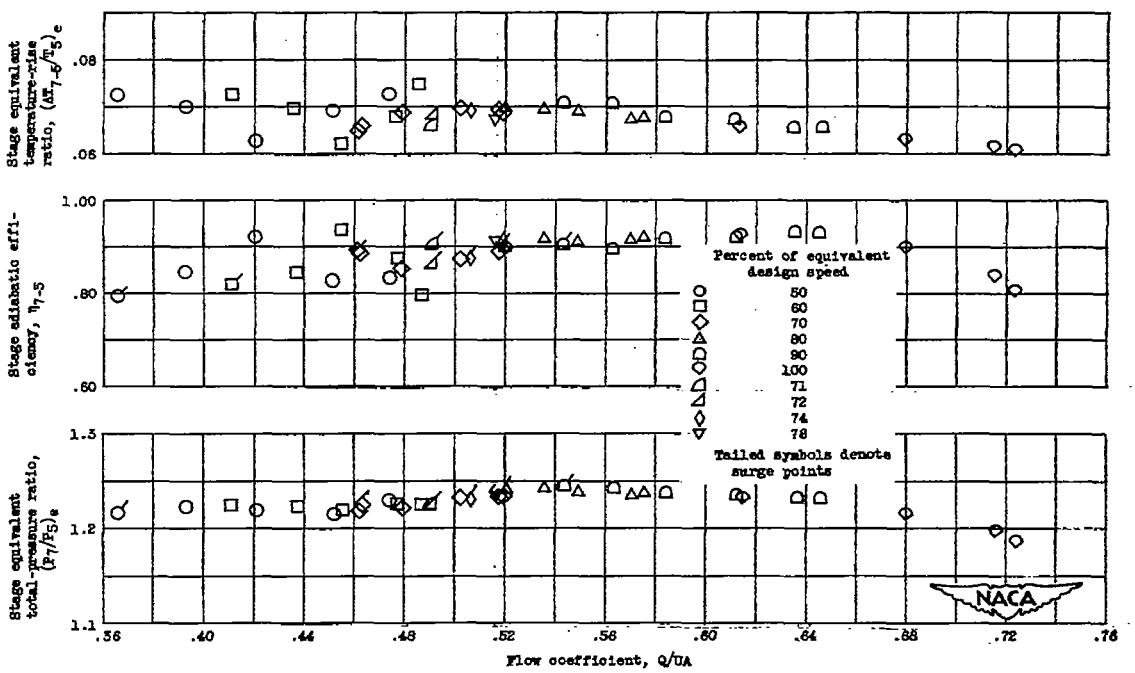

(c) Third stage.

Figure 6. - Continued. Individual stage performance of 10-stage compressor over entire flow range at speeds from 50 to 100 percent of equivalent design speed.

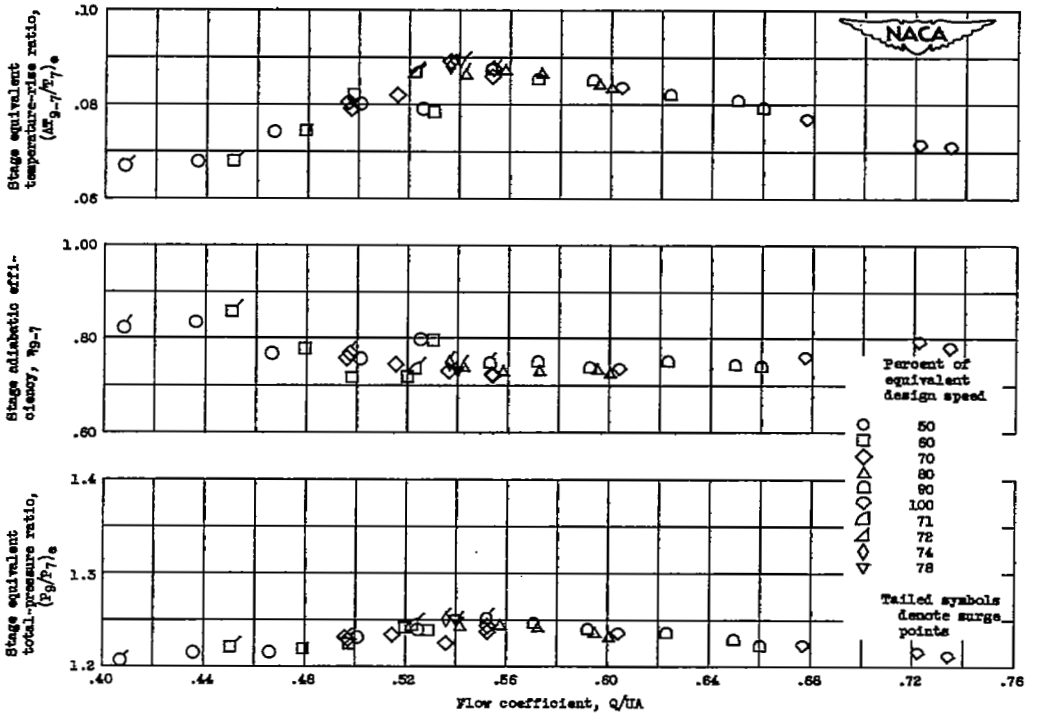

(d) Fourth stage.

Figure 6. - Continued. Individual stage performance of 10-stage compressor over entire flow range at speeds from 50 to 100 percent of equivalent design speed.

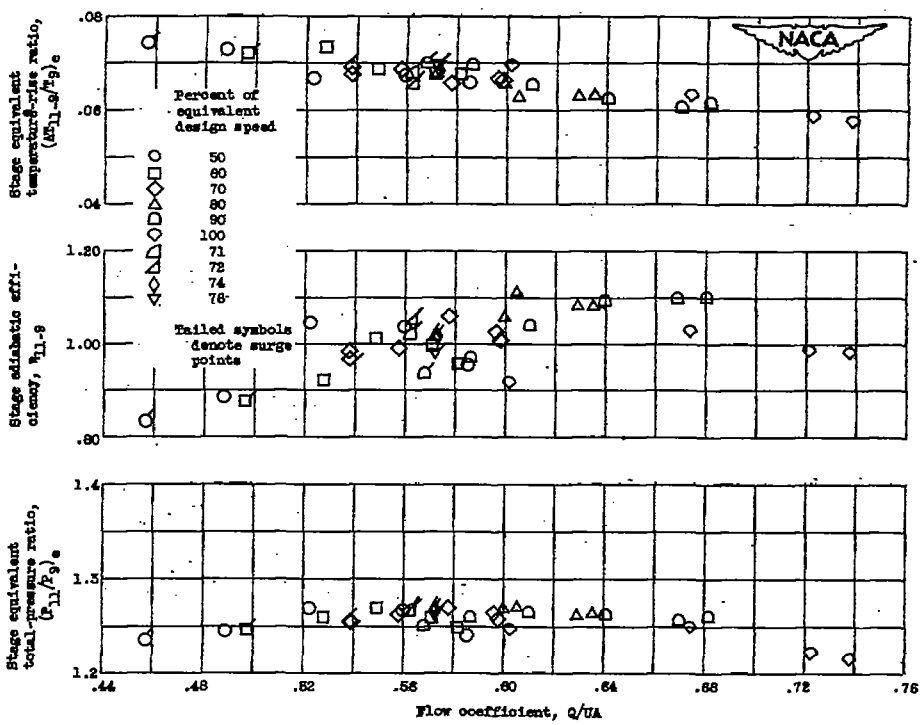

(e) Fifth stage.

Figure 6. - Continued. Individual stage performance of 10-stage compressor over entire flow range at speeds from 50 to 100 percent of equivalent design speed.

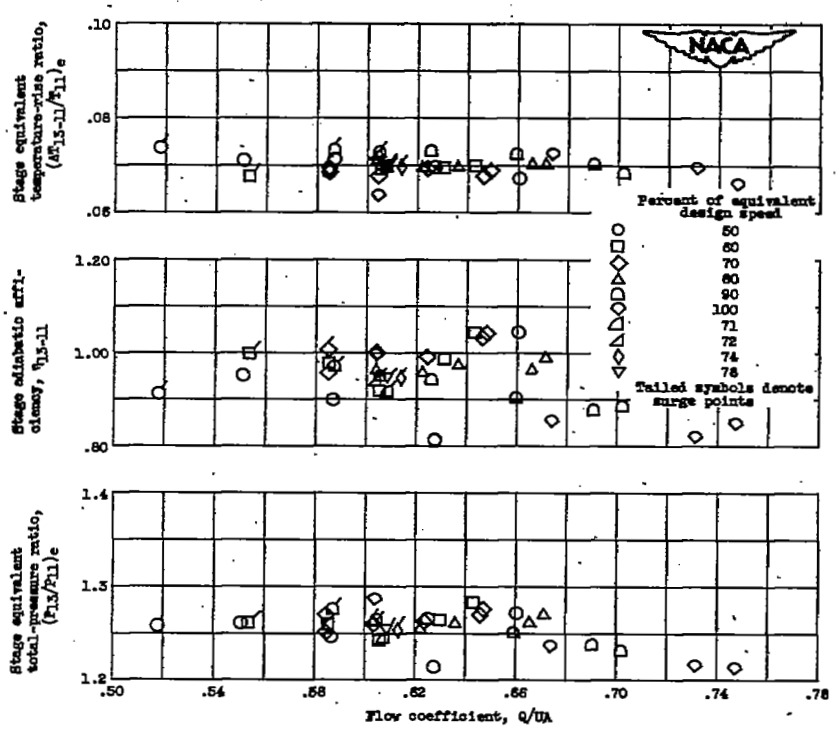

(f) Sixth stage.

Figure 6. - Continued. Individual stage performance of 10-stage compressor over entire flow range at speeds from 50 to 100 percent of equivalent design speed.

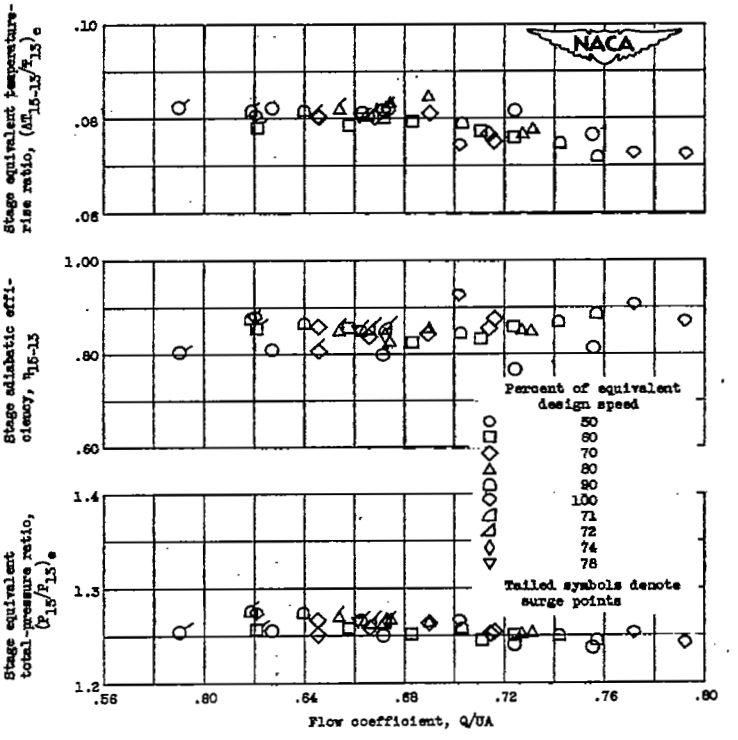

(g) Seventh stage.

Figure 6. - Continued. Individual stage performance of 10-stage compressor over entire flow range at speeds from 50 to 100 percent of equivalent design speed.

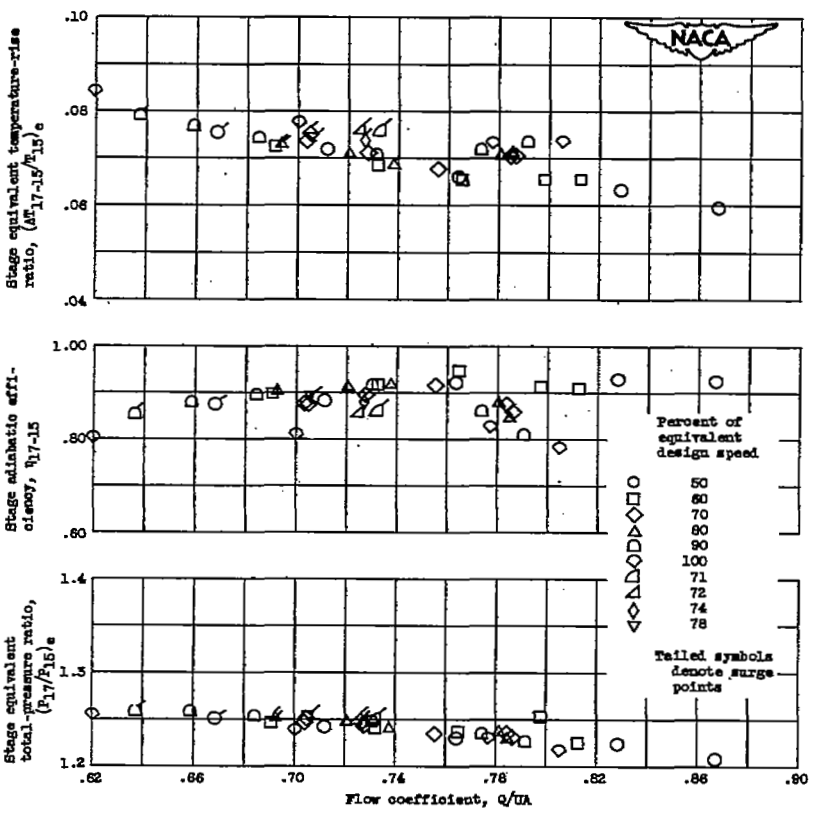

(h) Eighth stage.

Figure 6. - Continued. Individual stage performance of 10-stage compressor over entire flow range at speeds from 50 to 100 percent of equivalent design speed.

[redacted]

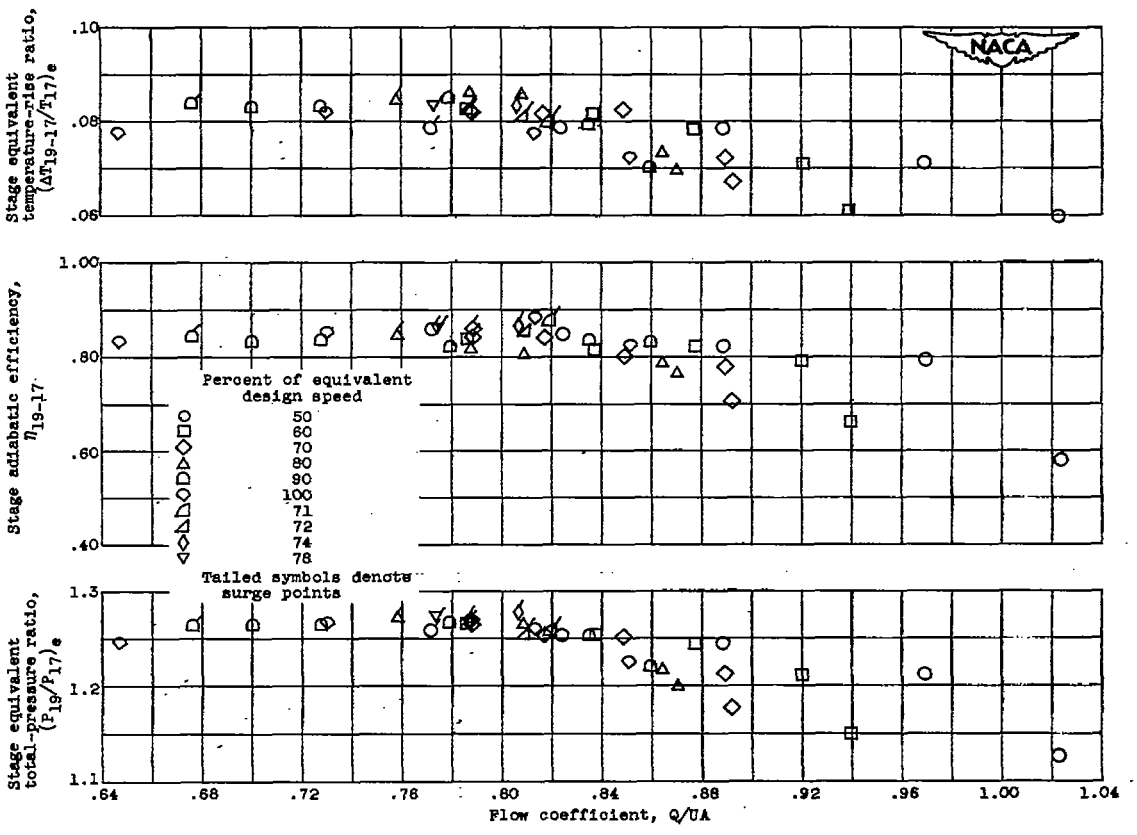

(i) Ninth stage.

Figure 6. - Continued. Individual stage performance of 10-stage compressor over entire flow range at speeds from 50 to 100 percent of equivalent design speed.

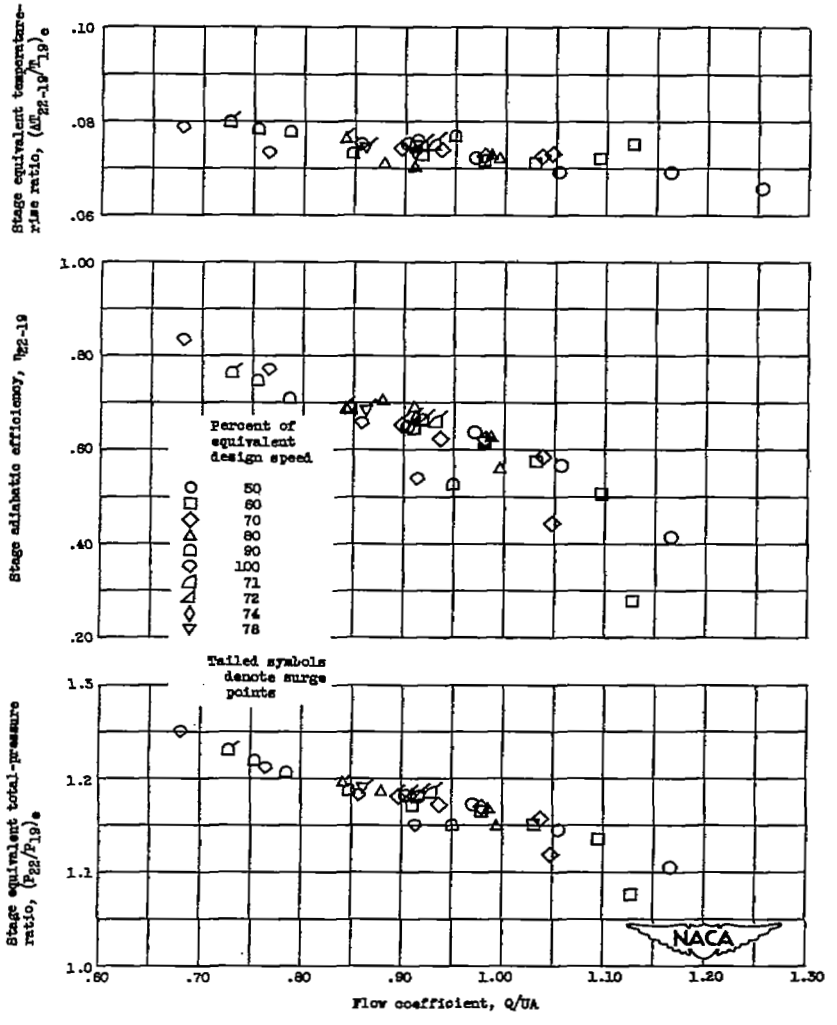

(j) Tenth stage.

Figure 6. - Concluded. Individual stage performance of 10-stage compressor over entire flow range at speeds from 50 to 100 percent of equivalent design speed.

[redacted]

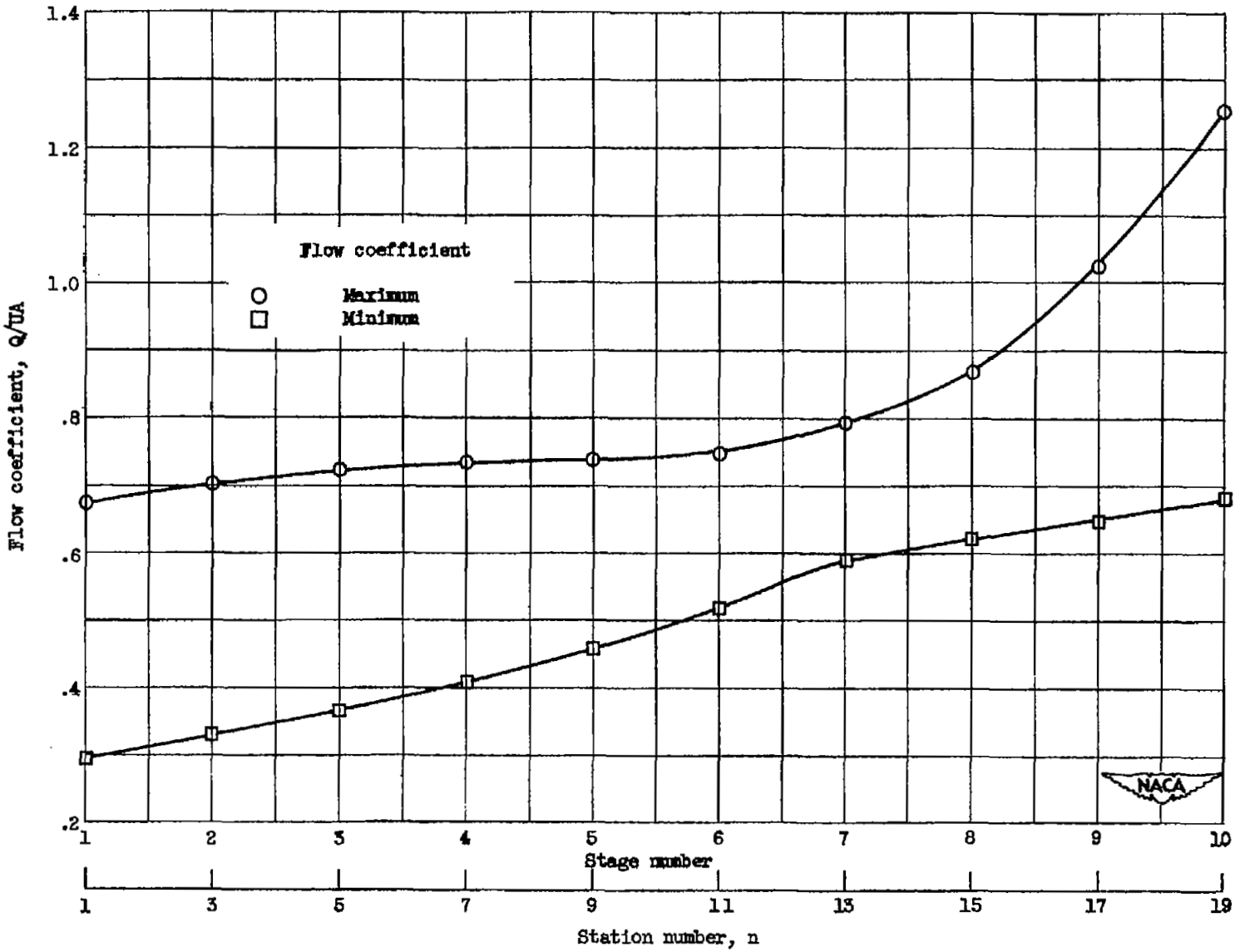

Figure 7. - Maximum flow coefficient range of individual stages from 50 percent of design to design speed.

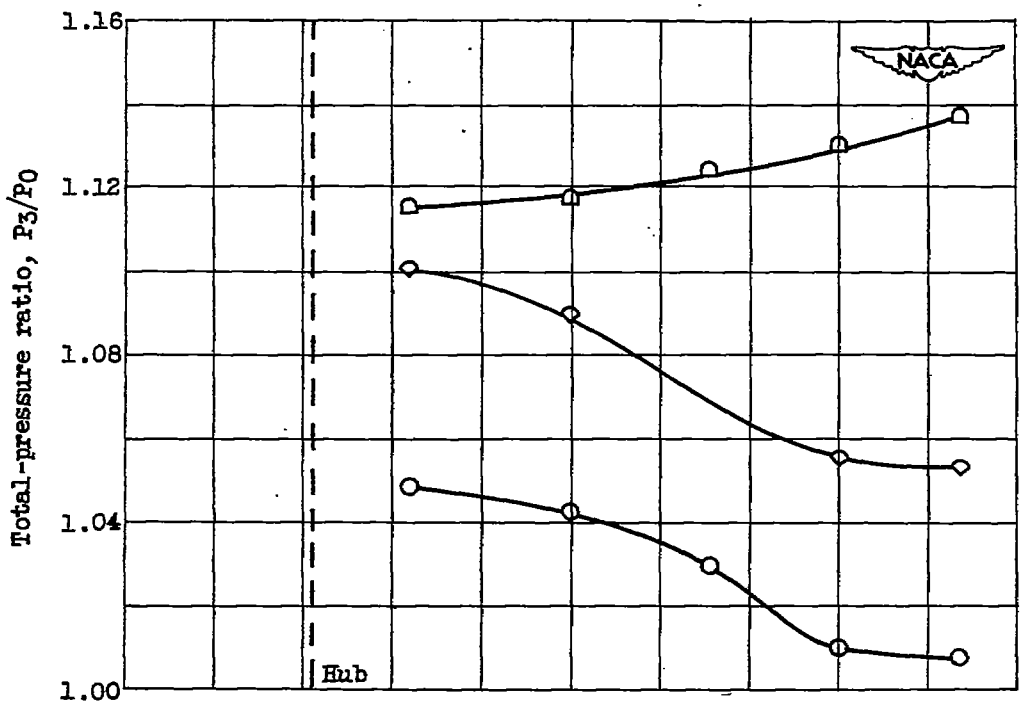

(a) Total-pressure ratio distribution.

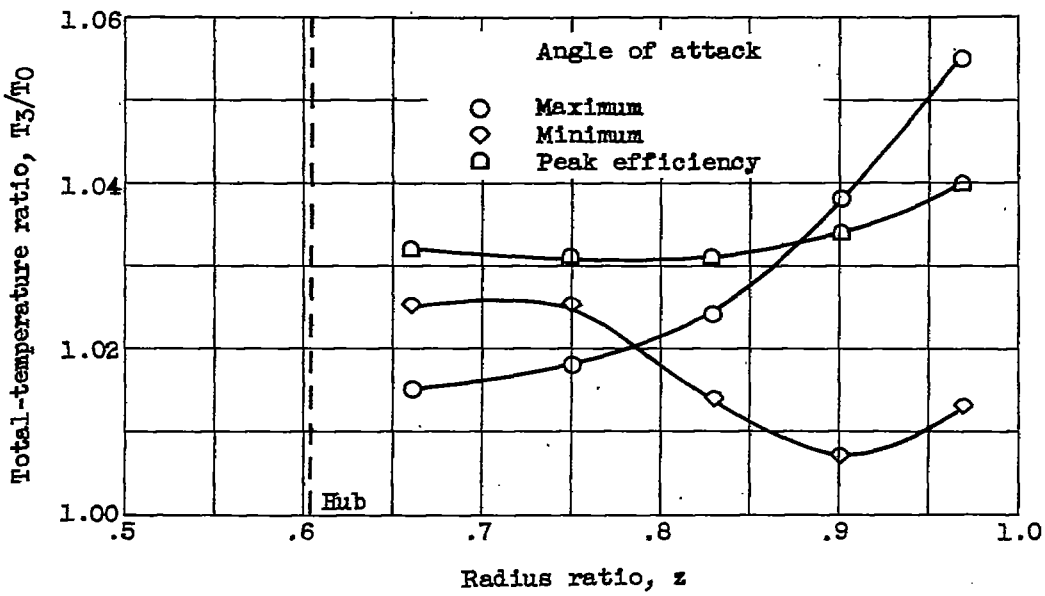

(b) Total-temperature ratio distribution.

Figure 8. - Radial distribution of inlet stage total-temperature and total-pressure ratios over a range of flow conditions.

[redacted]

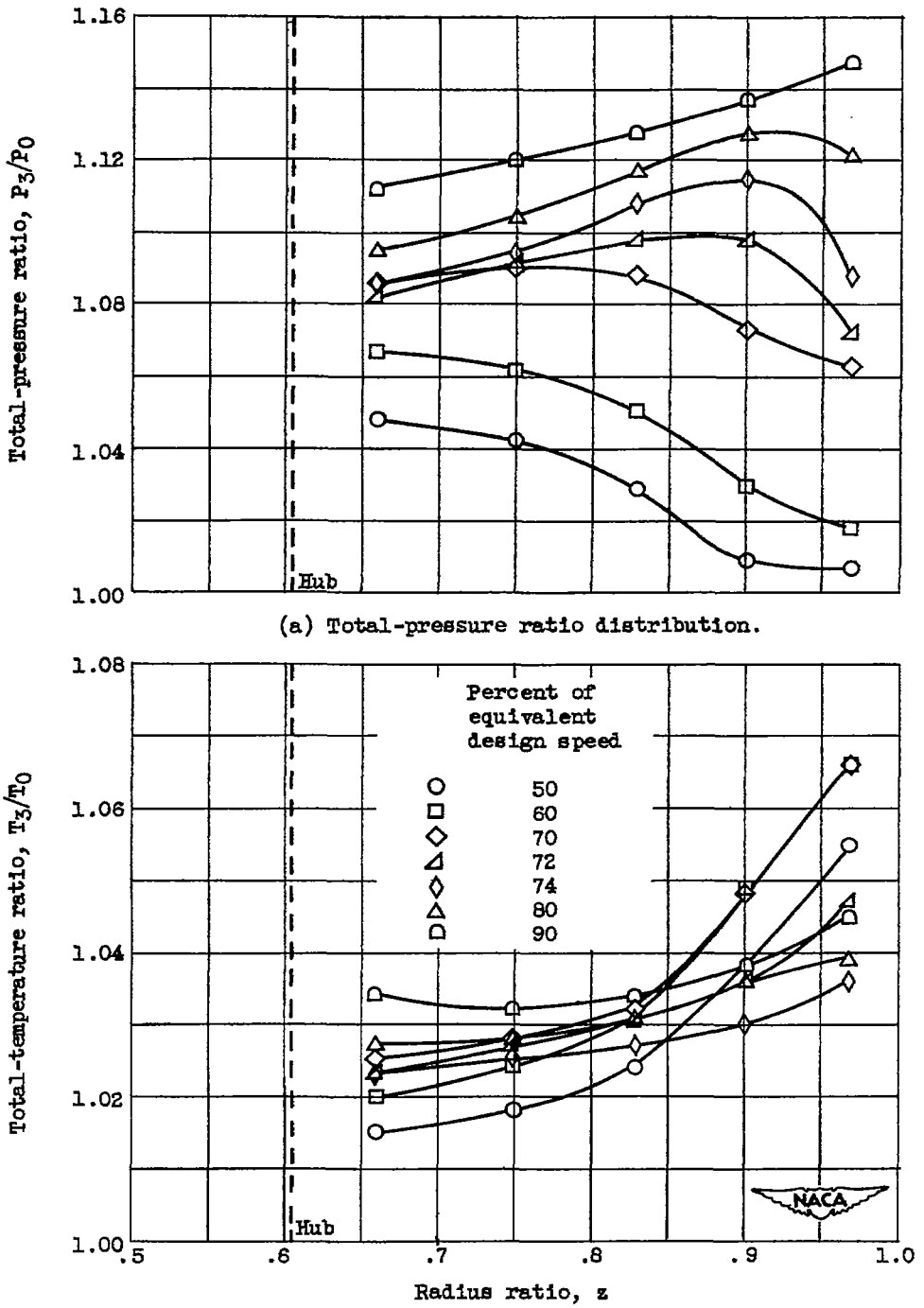

(a) Total-pressure ratio distribution.

(b) Total-temperature ratio distribution.

Figure 9. - Radial distribution of inlet stage total-pressure and total-temperature ratios at surge over a range of speeds.

[redacted]

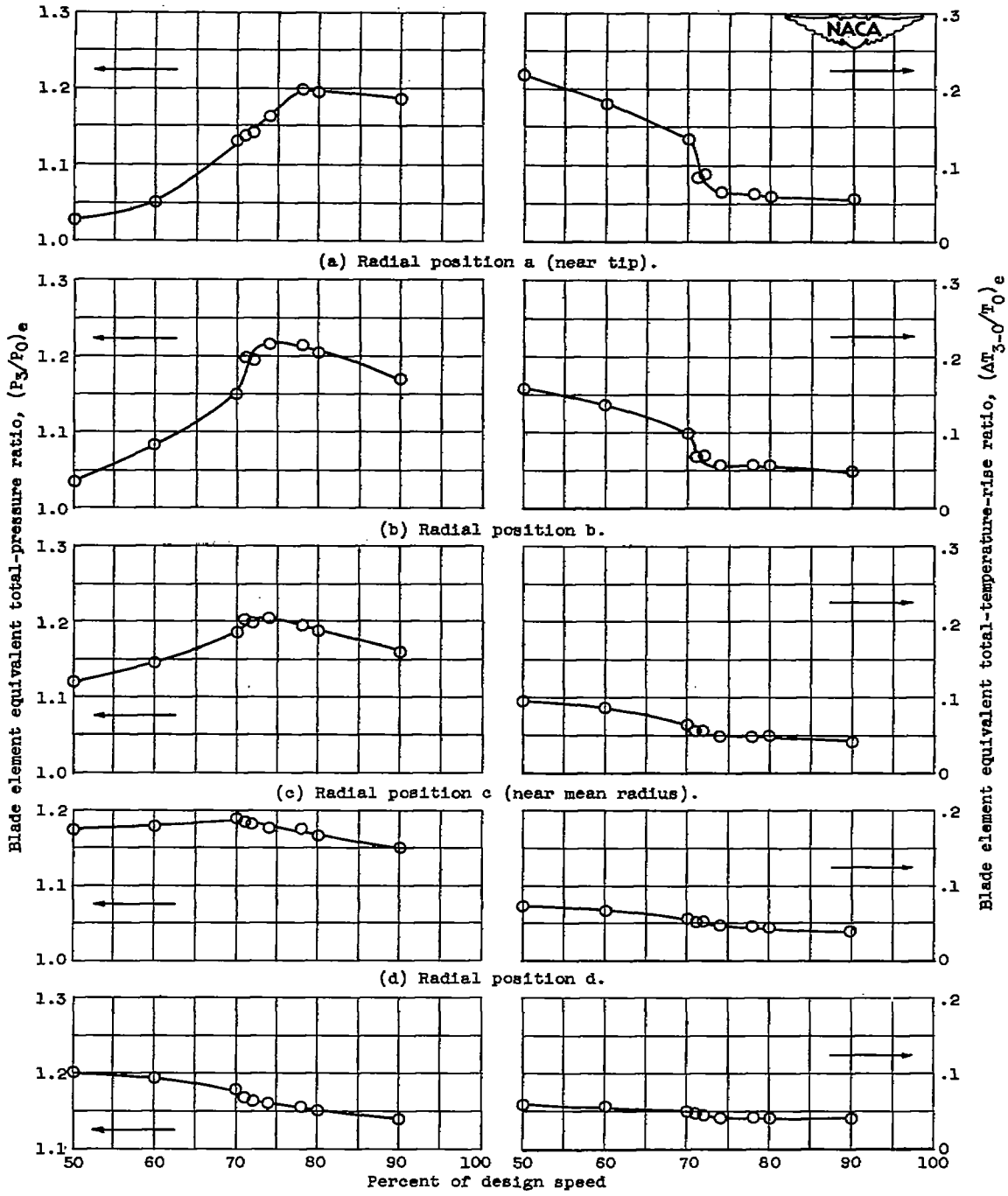

Figure 10. - Variation of inlet stage blade element equivalent total-pressure and total-temperature-rise ratios at surge over a range of speeds.

[redacted]

[redacted]